

Confluence-Associated Proliferation and Osteogenic Differentiation of Bone Marrow Mesenchymal Stem Cell (BMMSCS)

*Faten A.M. Abo-Aziza¹, Zaki A.A.²

¹Department of Parasitology and Animal Diseases, Veterinary Research Division, National Research Center (Cairo, Egypt).

²Department of Physiology, College of Veterinary Medicine, Cairo University (Giza, Egypt).
faten.aboaziza@gmail.com

Abstract: In the field of cellular therapy, the impact of confluence degree to harvest or differentiate BMMSCs and thereby the effect of microenvironment created by the increasing cell-to-cell contact remains controversial. Therefore, the effect of confluence on BMMSCs properties was studied and confluence-associated osteogenic differentiation efficiency was identified. The impact of confluences at 20, 50, 70, 80 and 100% on BMMSCs properties including cell viability, CFU-F, population doubling, Brd-U incorporation, expression of ERK and p-ERK proteins and glucose consumption rate was studied. Osteogenic differentiation efficiency was identified by determining calcium deposition, alizarin red staining, ALP activity and osteopontin and osteocalcin genes expression of the different confluent BMMSCs. There was a correlation between confluence % and the BMMSCs density. Viability was declined at the lower and higher confluences. The highest CFU-F, Brd-U uptake and population doubling were obtained when BMMSCs reached 80% confluence followed by decrease at 100% confluence. ERK band intensity in 100% confluent BMMSCs was lower compared to other confluences. Bands of p-ERK were highly detectable in 70% and 80% confluent BMMSCs. Glucose consumption rate at 70% and 80% confluences in the last days were higher than at 20% and 100% confluences. In spite of higher osteogenic differentiation estimated by calcium deposition, alizarin red stain and ALP activity at 80% confluences, it was also extended at 100% confluence. Osteopontin gene expressed among all confluences including 100% while osteocalcin gene was expressed highly in 70% confluent cells. We concluded that the optimum seeding density for maximal expansion and harvesting purposes is 80% confluence and up to 100% confluence for osteogenic differentiation to trigger the process more cost effective.

[Faten AM Abo-Aziza, Zaki AA. **Confluence-Associated Proliferation and Osteogenic Differentiation of Bone Marrow Mesenchymal Stem Cell (BMMSCS)**. *Stem Cell* 2016;7(3):43-56]. ISSN: 1945-4570 (print); ISSN: 1945-4732 (online). <http://www.sciencepub.net/stem>. 9. doi:[10.7537/marssci070316.09](https://doi.org/10.7537/marssci070316.09).

Keywords: BMMSCS, confluence, osteogenic differentiation, proliferation

1. Introduction

The interest in both the biological and potential therapeutic applications of the bone marrow adult stem cells is continuing (Prockop et al., 2003). Bone marrow mesenchymal stem cell (BMMSC) is adult stem cell has the capability to give rise to a variety of cells in the laboratory, including skeletal tissues, fat and muscle cells (Barry, 2003). Many studies aimed to culture BMMSC for a long period of time keeping their differentiation capacity in quantities proper to clinical applications, to be good candidates for tissue repair (Bittencourt and Aparecida, 2006).

In clinical purposes, extensive expansion of isolated BMMSCs in vitro is required to obtain adequate numbers of cells. However, most expansion protocols involved adherent culture on plastic surfaces and serial passage. Many variables were considered when optimizing BMMSCs expansion, among which cell confluence. Cell confluence is a critical factor because the degree of confluence might affect the biological properties of BMMSCs. Generally, BMMSCs are sub-cultured or harvested when they

reach a specified degree of confluence, but until now there is no standard concerning optimal confluence (Ren et al., 2015). For example, the using of different criteria to describe the conditions when the cells need to be sub-cultured, such as 50% to 60% confluence (Jeong et al., 2007 and Bae et al., 2009), 70% to 90% confluence (Tormin et al., 2009), sub-confluent (70% to 80%) (Lazarus et al., 2005), 80% confluence (Rosova et al., 2008 and Jones et al., 2010), 80% to 90% confluence (Grisendi et al., 2010), 90% confluence (Corcione et al., 2006), near confluence (Samuelsson et al., 2009), approaching confluence (Mankani et al., 2008) or confluent (Koc et al., 2000 and Zhukareva et al., 2010).

The outcomes of BMMSC from clinical trials were varied because BMMSCs used to treat many conditions are cultured to variable levels of confluence. Therefore, it is important to better understand how confluence at the time of harvest affects the properties of BMMSCs (Wolfe et al., 2008). For cell expansion under these circumstances, developing a measure to determine BMMSCs

confluence is in urgent need. As the optimal expansion of BMMSCs could be achieved by establishing the best seeding density and timing of passage and harvest to maintain consistent BMMSCs property (Ren et al., 2015).

Cells continuously receive clues from their environments by the activation of surface receptors and extra-cellular matrix. Inside the cells, it need to integrate diverse signaling pathways to trigger an appropriate biological response. One of these signal transduction molecules kinases is Extracellular signal-Regulated Kinase (ERK) (Kinnaird et al., 2004). ERK is involved in many fundamental cellular processes control such as cell proliferation, survival, differentiation, motility and metabolism (Gnecchi et al., 2005). ERK is activated by phosphorylation of both tyrosine and threonine residues (Iván et al., 2008 and Mandana et al., 2013). Activated ERK phosphorylates cytoplasmic, membranous and nuclear constituents and play a pivotal role in the regulation of many cell functions (Jean-Claude et al., 2007). Control of cell differentiation by activated ERK included stem cell commitment to chondrogenesis or osteogenesis under cyclic compression (Palaez et al., 2012), control of early osteogenesis by hydrostatic pressure (Liu et al., 2009), and stretch inhibition of adipogenesis (Lee et al., 2008). ERK plays an important role in the ECM-induced osteogenic differentiation process (Roman et al., 2004).

It was known that bone healing is highly complicated and regulated process. In certain positions, the normal bone repair and remodeling processes are often impaired such in non-union fractures and diseases including osteoporosis and osteoarthritis (Claes et al., 2012). Osteogenic progenitor cells have proved support in bone regeneration when they were locally transplanted into bone defects as well as poorly or non-healing fractures. Therefore, osteogenic MSC preparations have been used as new cell-based therapies needed to repair damaged skeletal tissues (Chandrasekhar et al., 2011). For the detection of osteogenic differentiation, it was necessary to use alizarin red stain (Wen et al., 2014), alkaline phosphatase activity (Kentaro et al., 2012) and/or determine some genes expression like osteocalcin and osteopontin (Cho et al., 2014). Therefore, the present work aim to explore the 20, 50, 70, 80 and 100% confluences on BMMSCs proliferation capacity and their osteogenic differentiation efficiency.

2. Material and Methods

2.1. Animals

Three months old male rats weighted 175 – 200 gm were used. All experiments on animals were performed under the institutionally approved

protocols for the use of animal research.

2.2. Isolation and Cultivation of rat bone marrow mesenchymal stem cells (BMMSCs)

To isolate BMMSCs, femurs bone from rats were isolated (Lilian et al., 2009). Skin incision was made with a scalpel in the femoral epiphysis region and the muscle was sectioned up to the femoral bone. Femurs bone from rats were isolated and flushed using PBS. Standardised osteotomy was created at the femurs head as described previously (Röntgen et al., 2010). Bone marrow was aspirated with a 5-ml syringe containing 5000 UI/ml of heparin. The total volume of bone marrow blood (2ml) from femurs was used for mononuclear cell isolation by gradient centrifugation at 2000 rpm for 30 minutes at room temperature on same volume of Ficoll-Histopaque®-1077-Sigma. Then the mononuclear cell layer was aspirated with a pipette, washed twice and suspended in alpha minimum essential medium (α -MEM, Invitrogen, Grand Island, NY, USA). After counting the cells with haemocytometer, the single suspension of bone marrow derived all nucleated cells were seeded at a density of 15×10^6 into 100 mm culture dishes (Corning, USA) and incubated at 37°C and 5% CO₂. After two days, the media was changed to remove non-adherent cells while the attached cells were maintained in α -MEM supplemented with 20% fetal bovine serum (FBS, Equitech bio, Kerrville, TX, USA), 2 mM L-glutamine, 55 μ M 2-mercaptoethanol, 100 U/ml penicillin, and 100 μ g/ml streptomycin (Invitrogen) (Chandrasekhar et al., 2011). The media was changed every 3 days thereafter until the colonies reached 20, 50, 70, 80 and 100% confluence as determined by microscope observation. The cells were harvested and designated as passage 1, and serial passage numbers were designated thereafter. The cultured BMMSCs of passage 3 were plated to the T-25 flask from identified confluence for further culture. When passage 3 BMMSCs reached the respective confluences, they were harvested (passage 4) and subjected for cell proliferation and differentiation as follow:

2.2.1. Cell counting and viability assay

Upon reaching 20, 50, 70, 80 and 100% confluence, BMMSCs from each confluence were washed with 10 mL of PBS twice, digested with 1 mL of Trypsin (Invitrogen, Life Technologies) and centrifuged at 2000 rpm for 5 min. The cell number was then counted and viability was assessed by use of the trypan blue exclusion method (Lilian et al., 2009).

2.2.2. Colony forming unit-fibroblastic (CFU-F) assay

One million cells of the BMMSCs Upon reaching 20, 50, 70, 80 and 100% confluence were seeded on a T-25 cell culture flask (Nunc, Rochester, USA). The cultured cells were washed with PBS after

16 days, and then stained with 1% toluidine blue solution in 2% paraformaldehyde. After microscopical examination, each cell cluster that contain more than 50 cells was considered as a colony (**Chandrasekhar et al., 2011**). The colonies number was counted in five independent samples per each confluence group.

2.2.3. Cell proliferation assay

The proliferation of each confluent BMMSCs was created using the bromodeoxyuridine (Brd-U) incorporation assay (**Chandrasekhar et al., 2011**). For each confluence, 1×10^4 cells/well was seeded on two-well chamber slides (Nunc) for 2-3 days. The cultured wells were incubated with Brd-U solution (1:100) (Invitrogen) for 24 hours, and then stained with a Brd-U staining kit (Invitrogen). Total and positive Brd-U cell numbers were counted in five images in each confluence.

2.2.4. Population doubling assay

Population doubling (PD) and population doubling time (PDT) were calculated by use of the method described previously (**Ren et al., 2015**). A total of 0.25×10^6 cells of BMMSCs from each confluence were seeded on 60 mm culture dishes. The cells were passaged upon reaching 20, 50, 70, 80 and 100% confluence. The number of BMMSCs at every passage was counted and the PD in each passage was calculated using equation: \log_2 (harvested cells number/ plated cells number). The final PD for each confluence were determined by cumulative addition of total numbers in each passage until the cell division was ceased. The population doubling time (PDT) for each confluence was monitored in Passage 5 to 6 and in Passage 11 to 12, respectively.

2.3. Western blotting analysis

Protein was extracted from cells as previously described (**Tahrin et al., 2012**). The adhered cells were washed with Dulbecco's phosphate-buffered saline and dislodged by cell scraper. Cells were collected into tubes and centrifuged at 1500 RPM for 5 minutes. Then the cells were lysed with 180 μ L of ice cold cell lysis buffer and 20 μ L fresh protease inhibitor cocktail (Haltä, Pierce) for 30 min on ice followed by 10 min centrifugation at 12,000 RPM, at 4°C to clarify the lysate. The supernatant (or protein mix) was transferred to a fresh tube and stored on ice or frozen at -20°C or -80°C. Protein concentrations were measured spectrophotometry. ERK and p-ERK were measured in 20, 50, 70, 80 and 100% confluent BMMSCs (**Tain-Hsiung et al., 2007**). Sample cells was prepared by being heated for 5 min at 95 °C in a sample buffer and equal aliquots were then run on prepared 10% SDS-polyacrylamide gel. Proteins were transferred to PVDF membrane filters and then blocked with 5% skim milk in TBST for 1 h. After that membrane filters were incubated overnight at 4 °C with the primary antibodies against ERK and p-

ERK (Cell Signaling Technology). The membranes were washed and the primary antibodies were detected by incubating with horseradish peroxidase-conjugated goat anti-rabbit or anti-mouse IgG (PharMingen) respectively. The filters were washed and developed using a chemiluminescence system (ECL, Amersham Biosciences, UK). β -actin on the same membrane was served as the loading control and the immunoreactive bands were then visualized. Bands intensities were quantitatively analyzed by using IMAGEJ software and normalized relative to corresponding control β -actin for each protein and p-ERK related to ERK were calculated.

2.4. Glucose consumption test

For monitoring BMMSCs markers of confluence, glucose was measured in BMMSCs culture supernatants that indicating glucose consumed by BMMSCs isolated from different confluence as previously described by **Waters et al. (2003)**. One million cells of each confluence was cultured in 100mm culture dishes and supplemented with 10mg glucose/ml. The concentrations of glucose were estimated daily in the culture supernatant of BMMSCs using glucometer. The consumption was estimated as the quantity of glucose (mg/ml) consumed minus the concentration of cell culture at beginning.

2.5. In vitro osteogenic differentiation assay

BMMSCs from each confluence were cultured under osteogenic culture conditions (**Chandrasekhar et al., 2011**). BMMSCs were induced for 14 days in α -MEM with 20% FBS, 2 mM L-glutamine, 55 μ M 2-ME, 100 μ M L-ascorbic acid 2-phosphate, 2 mM β -glycerophosphate, 10 nM Dexamethasone, 100 U/ml penicillin and 100 μ g/ml streptomycin. The medium was changed every 3 days. Confirmation of osteogenesis was done by means of alizarin red staining (to highlight ECM calcification), calcium deposition assay, assessment of ALP activity, and expression of osteopontin and osteocalcin genes.

2.5.1. Alizarin red staining

After 4 weeks of culture in osteogenic condition, the cells were stained for extracellular mineralization as described by **Arash et al. (2008)**. The cells in 60mm dishes were washed with PBS and fixed in 60% (v/v) isopropanol (Sigma-Aldrich). After 1 min the cells were rehydrated with distilled water then alizarin red stain 1% (pH 4.1, Sigma-Aldrich) was added to each dish. The dishes were incubated at room temperature for 3 min and then they were washed four times with distilled water and leaved in air to dry. Finally, the % of total area alizarin stain was read in triplicate at 405 nm in 96-well format using opaque-walled, transparent- bottomed plates (**Gregory et al., 2004**).

2.5.2. Calcium Assay

The differentiation of osteoblasts was

determined by calcium assay as described elsewhere by **Salasnyk et al. (2004)**. Briefly, fixed quantities from each confluence were seeded into wells and washed twice with PBS and extracted off the wells in 0.5 N HCl. Accumulated calcium was removed from the cellular component by shaking for 5 h at 4°C, followed by centrifugation at 2,000 g for 10 min. The supernatant was utilized for calcium determination using calcium colorimetric assay kit (Sigma-Aldrich). Total calcium was calculated from standard solutions prepared in parallel and expressed as mg/well after absorbance at 575 nm was measured.

2.5.3. Alkaline Phosphatase (ALP) activity

The differentiation of osteoblasts was

determined by ALP activity assay as described elsewhere by **Liu et al. (2003)**. Briefly, the cells were treated with 20 $\mu\text{L}/\text{well}$ 0.1% Triton X-100 (Sigma-Aldrich) for 5 min at room temperature for cell lysis. 100 $\mu\text{L}/\text{well}$ of the ALP assay kit (Sigma-Aldrich) was then added to produce p-nitrophenol from the hydrolysis of p-nitrophenyl phosphate. The ALP activity of cell lysates was determined by measurement of absorbance at 405 nm caused by p-nitrophenol using a MRX Microplate Reader.

2.5.4. Reverse Transcriptase-Polymerase Chain Reaction (RT-PCR)

Table 1. Primers used for RT-PCR

Gene name	Primer sequences	Product size (bp)
SSP1 (Osteopontin)	Forwards 5' -AGACCCAAAAGTAAGGAAGAAGA-3' Reverse 5'-GACAACCGTGGGAAAACAAATAAG-3'	564
BGLAP (Osteocalcin)	Forwards 5' -CGCAGCCACCGAGACACCAT-3' Reverse 5'- AGGGCAAGGGGAAGAGGAAAGAA-3'	400

RNA was isolated from 10×10^6 osteogenic BMMSCs differentiated from each confluence. the RNeasy mini kit (Qiagen, Valencia, CA) was used for total RNA isolation. RT-PCR was carried out with the One Step RT- PCR Kit (Qiagen) and a 96 well thermal cycler using primers specific for osteopontin and osteocalcin listed in Table1. For each reaction one microgram of template RNA was used. The reverse transcription step was allowed to run for 30 min at 50°C, followed by PCR activation for 15 min at 95°C. Then thirty amplification cycles were run with one min at 94°C, 58°C and 72°C of denaturation annealing and extension respectively. After that final extension was run 10 min at 72°C. The products were separated by gel electrophoresis using a 1% agarose gel. Bands were visualized using UV illumination of ethidium-bromide-stained gels and were captured using Gel imaging system.

2.5. Statistical Analysis

Data were analyzed with the Statistical Package for the Social Sciences version 19 (SPSS-19).

3. Results

3.1. Light microscopy images

The light microscopically examination showed that BMMSCs appeared 20% confluence after 2-3 days in culture but after 2 weeks they became 50% confluence and after 2-3 weeks they became 70% confluence while they became 80% and 100% after 3-4 weeks. All BMMSCs among all confluent cells exhibited spindle-shaped morphology. BMMSCs appeared large and flattened in culture at 20, 50 and 70% confluence, but when BMMSCs reach 80% and

100% they became very confluent and lined next to each other (Figure 1).

3.2. Cell density

BMSCs were cultured to 20, 50%, 70, 80 and 100% confluent; the cell densities per cm^2 culture area were calculated. it was found that higher BMMSC density correlated with increased confluence. It was found that the highest cell density appeared when the cell achieved 100% confluence (4.802×10000 cells/ cm^2) and the lowest density appeared at 20% confluent BMMSCs (1.089×10000 cells/ cm^2) while it was 2.887×10000 cells/ cm^2 and 3.679×10000 cells/ cm^2 at 70% and 80% confluent cells respectively which is significantly lower than that at 100% confluent and higher than other confluent BMMSCs (Figure 2A).

3.3. Cell viability

The viability was less than 90% in all confluent cells except higher viability at 70% that recorded 90.71%. There was no significant difference in viability among 50%, 70% and 80% confluent cells. BMMSCS viability decline at 20% and 100% confluent cells and no significant difference between them (84.16% and 85.67%) respectively (Figure 2B).

3.4. CFU-F

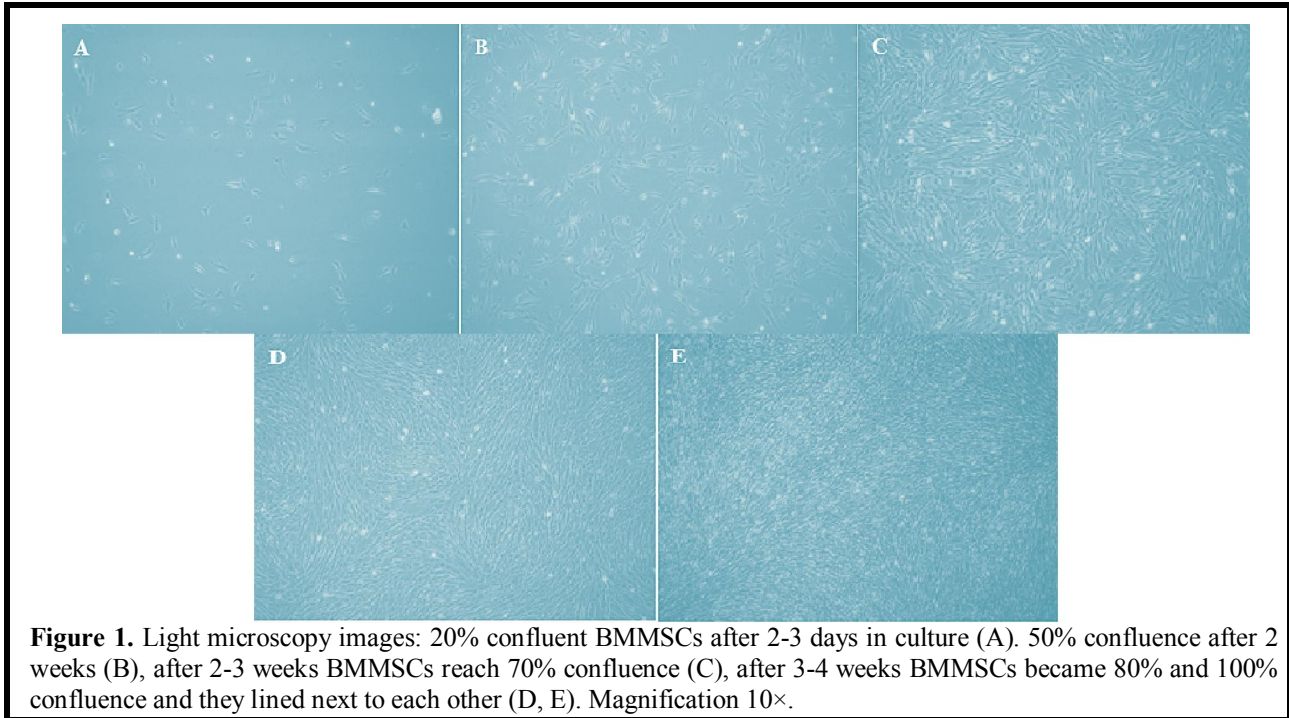
As the confluence of BMMSCs increase until reach 80% the cells become highly adhered to the BMMSC-ECM and form CFU-F at a high extent, and then decreased with increasing the confluence to 100% (Figure 2C).

3.5. Cell proliferation assay

The Proliferation rates of BMMSCs at different confluent cells were assessed by Brd-U incorporation for

24 hours. The Brd-U uptake rate is significantly elevated as the confluence increased until reach the higher at 80% confluence. It was appeared that the percentage of positive cells is significantly higher

(56.25% and 63.48%) in 70% and 80% confluent BMMSCs compared with 20%, 50%, and 100% confluence (31.82%, 39.43% and 16.56%) respectively (Figure 3A).



3.6. Population doubling

The PD was calculated at every passage according to the equation: \log^2 (number of harvested cells/number of seeded cells). For all confluences, comparison of final PD score indicates maximal expansion potential, BMMSCs among 70% and 80% confluences exhibit a significant increase in PDs when compared to that at 50% and 100% confluences (Figure 3B). Population doubling time (PDT) was recorded in Passage 5 to 6 and in passage 11 to 12, respectively. In both passages, the PDT of 70% and 80% confluent BMMSCs was slightly shorter than 50% confluent cells but much shorter than 20% and 100% confluent cells (Figure 3C). BMMSCs at 70% and 80% confluence showed highly PD score than other confluences in all passages. All confluent BMMSCs showed maximal expansion potential in passage 3-4. In most confluent BMMSCs, cell growth arrested in Passage 12-13, whereas 70% and 80% confluent stopped in Passage 14-16 (Figure 3D).

3.7. The expression of ERK and P-ERK proteins

The expression of ERK and p-ERK proteins was performed by Western blotting using anti ERK and p-ERK antibodies respectively. As shown in figure 4, bands of ERK were expressed in BMMSCs and detectable by Western blot among all the confluences.

Bands of p-ERK were highly detectable in 70% and 80% confluent BMMSCs than other confluences (Figure 4A). Densitometric measures of band intensities for ERK and p-ERK using IMAGEJ software and B-actin was used as control. It was found that ERK band intensity of 100% confluent BMMSCs was lower compared to other confluences. The intensities of remaining confluences bands were nearly the same. While the higher p-ERK band intensity was found in 70% and 80% confluent BMMSCs compared to other confluences (Figure 4B). Phosphorylation of ERK (p-ERK) in 80% confluent BMMSCs was much higher than 20% and 50% confluent cells but slightly higher than 70% and 100% confluent cells. Phosphorylation of ERK in 70% and 100% was higher than 20% and 50% confluences (Figure 4C).

3.8. Glucose consumption rate

For monitoring activity of BMSC confluences, we measured glucose of the BMSC culture supernatants. The concentrations of glucose were estimated daily in the culture supernatant of BMSC using glucometer. It estimated as the quantity of glucose (mg/ml) consumed minus the concentration of cell culture at beginning. The glucose levels decreased daily despite small fluctuations after medium change

on days 4, 5 and 6. All BMMSs in all confluence are regular in glucose consumption after day 2. However, on days 3, 4 and 6, glucose consumption of BMMSCs at 70% and 80% confluence was elevated than the others. On the day 5 the consumption rates of BMMSCs at confluence 50, 70, and 80% were higher than the lowest (20%) and highest (100%) confluences (Figure 5).

3.9. Osteogenic differentiation

To address whether confluence affects osteogenic differentiation of BMMSCs, % of total area of Alizarin Red staining, calcium deposition and the activity of alkaline phosphatase (ALP) were determined. Cells cultured in 20% and 50% did not cause a significant increase in % of total area of Alizarin Red staining as compared with the cells cultured at 70, 80 and 100% confluence (figure 6a). % of total area of Alizarin Red staining of both 80% and 100% confluent BMMSCs are significantly higher

than that in the other confluences. Measurement of calcium deposition resulted in a significant increase in OD in MSCs cultured at 80% confluence than both 70% and 100% confluence. However, MSCs cultured in 100% confluence further increased the OD value of ALP activity than the other confluence (Figures 6b).

3.10. Osteopontin and osteocalcin gene expression

The effect of confluence on osteogenic gene expression was measured by RT-PCR analysis of osteopontin and osteocalcin expression with gene specific primers on cells of different confluences. It was found that BMMSCs derived osteogenic cells expressed prominent osteopontin gene among all confluences. In contrast, osteocalcin gene expression was abundant in 70% confluent cells than other confluent cells. In addition, 100% confluent cells showed abundant osteocalcin expression than 20, 50 and 80% confluences (Figure 7).

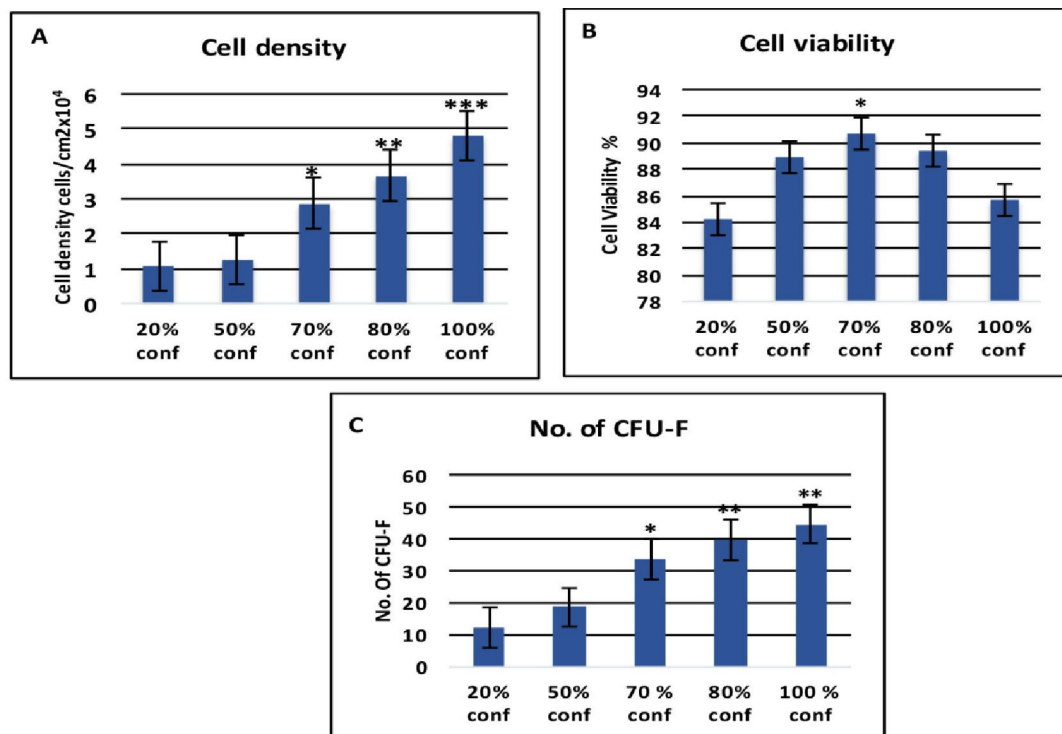
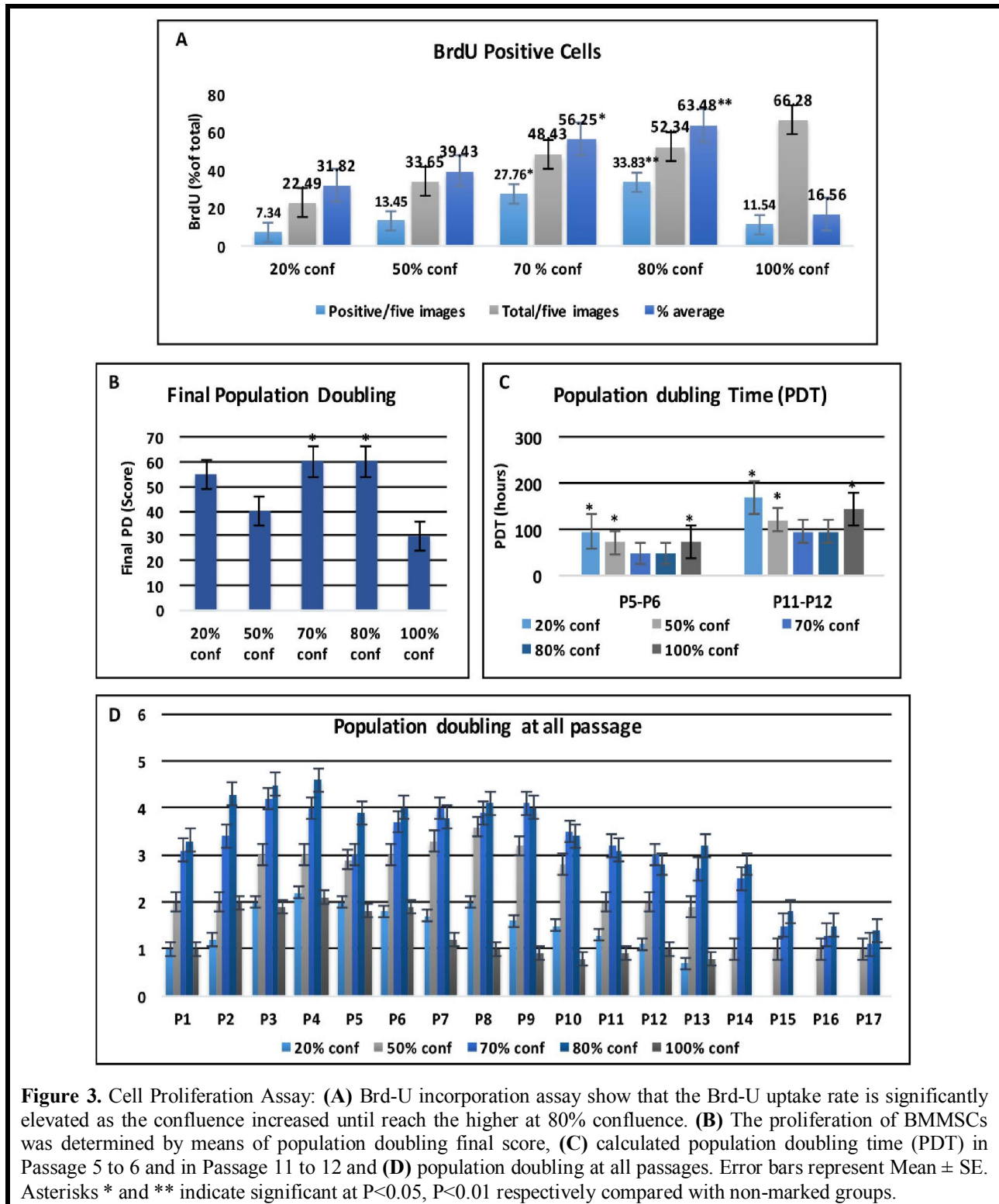
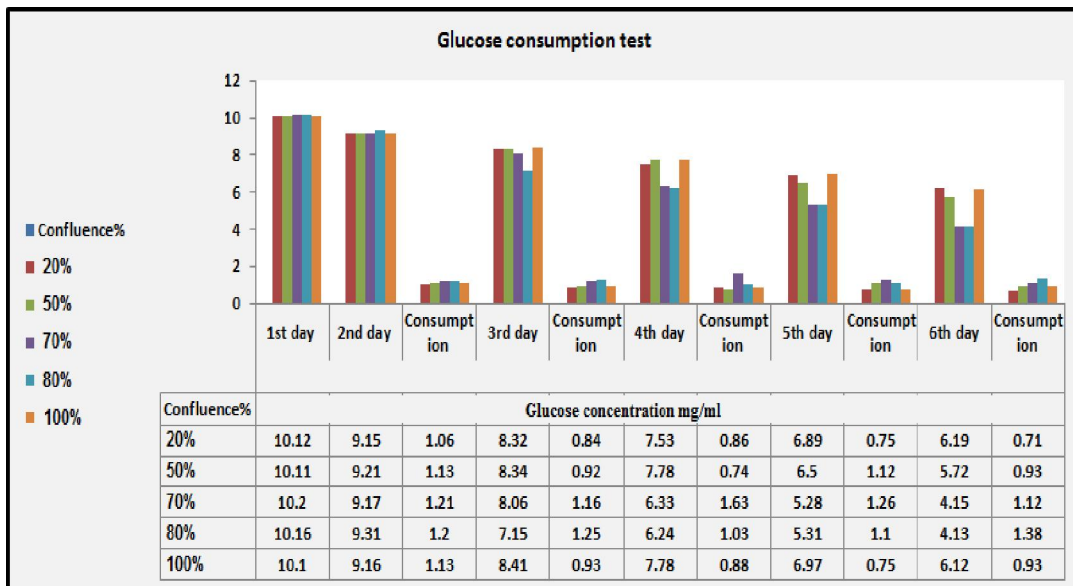
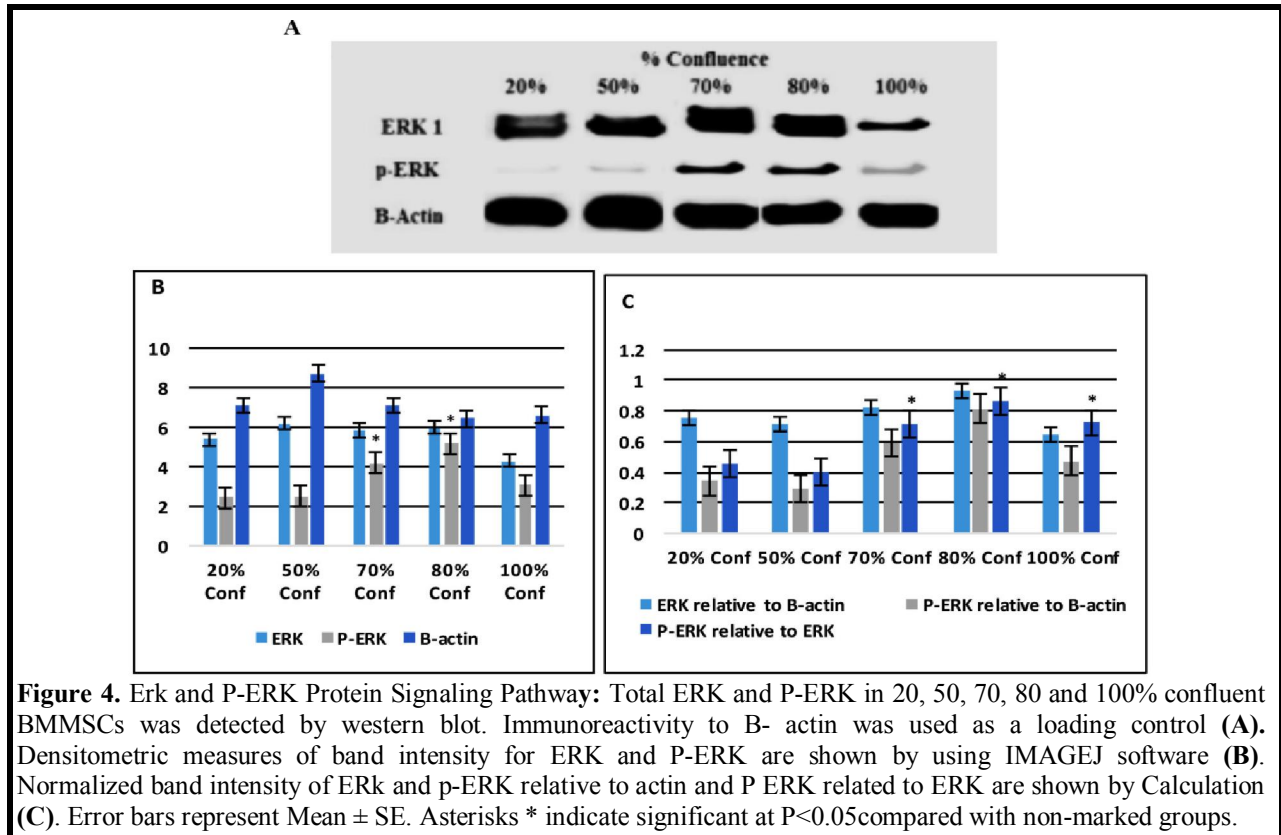


Figure 2. (A) Cell Density: The highest cell density appeared in 100% confluence (4.802×10^6 cells/cm²) and the lowest density appeared in 20% confluent BMMSCs (1.089×10^6 cells/cm²). **(B) Cell viability:** The viability was less than 90% in all confluences except higher viability at 70% that recorded 90.71%. There was no significant difference in viability among 50%, 70% and 80% and declined at 20% and 100% confluences. **(C) Cell Forming Unit- Fibroblastic:** The number of plastic attached CFU-F from BMMSCs up on reaching 20, 50, 70, 80 and 100% confluences (1×10^6 cells). The highest number of CFU-F was in 80% confluence and then decreased with increasing the confluence to 100%. Error bars represent Mean \pm SE. Asterisks *, ** and *** indicate significant at $P < 0.05$, $P < 0.01$, $P < 0.001$ respectively compared with non-marked groups.





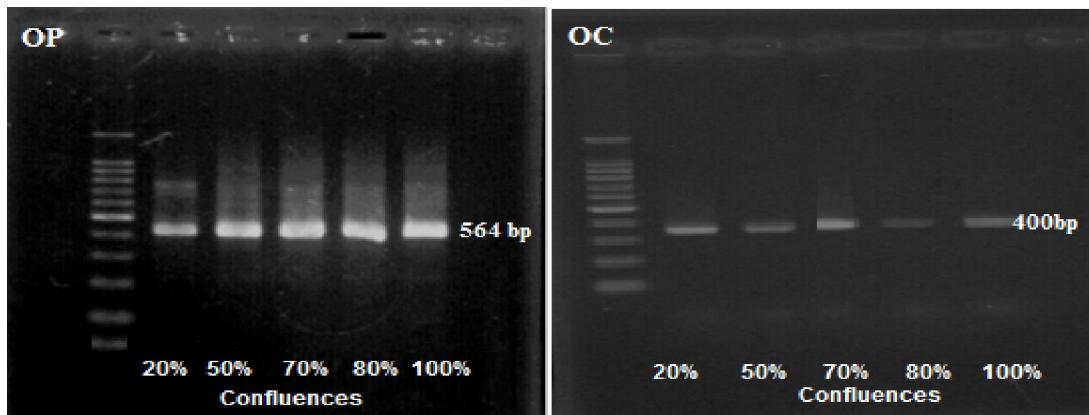
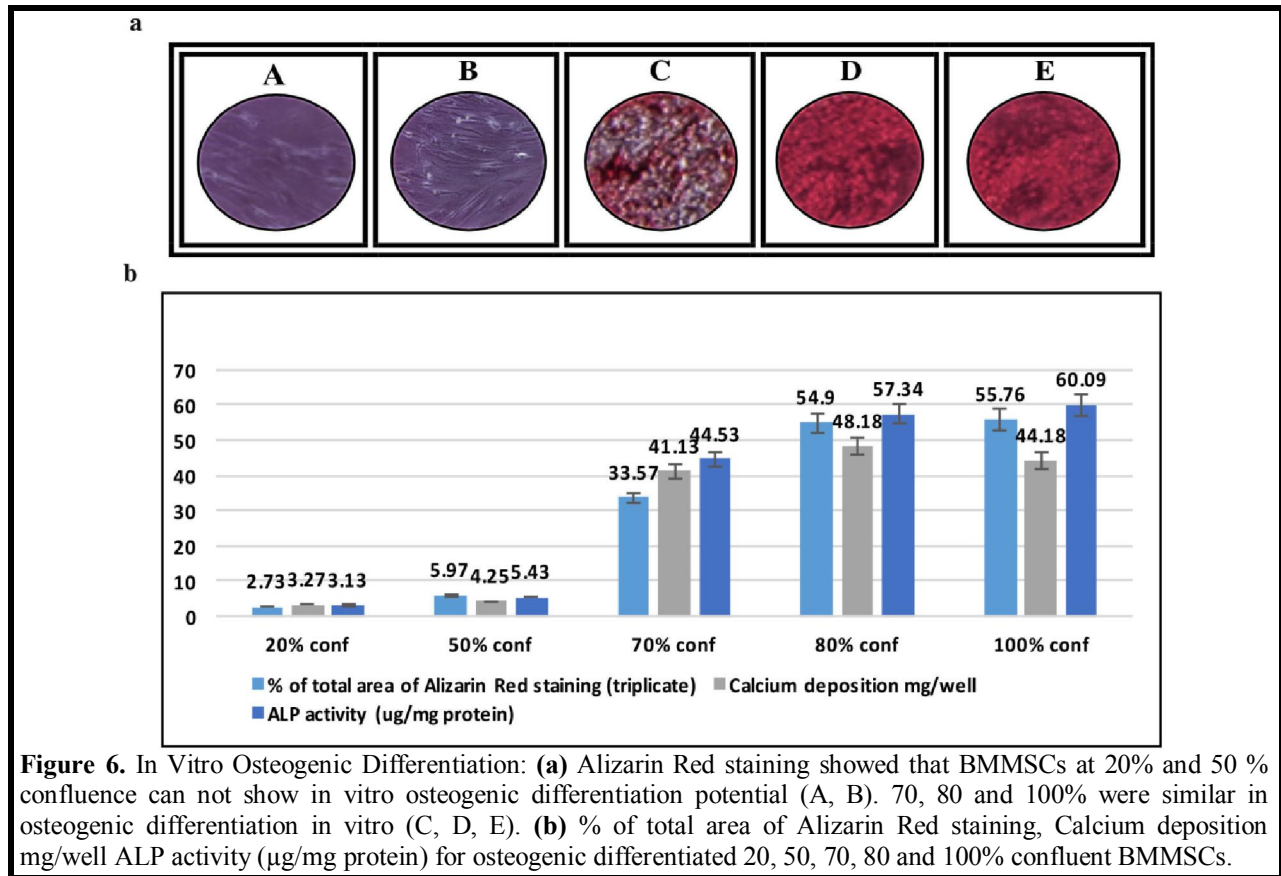


Figure 7. RT-PCR analysis of osteopontin (OP) and osteocalcin (OC) expression with gene specific primers on cells of 20, 50, 70, 80 and 100% confluent BMMSCs.

4. Discussions

In the field of cellular therapy, the degree of confluence at which to passage or harvest BMSCs remains an important silent factor. Therefore, the effects of confluence on BMSCs properties was studied and confluence-associated osteogenic differentiation efficiency was identified. This study reflect the impact of cell density and microenvironment created by the increasing cell to cell contact on cell viability, CFU-F, population

doubling, Brd-U incorporation, expression of ERK and P-ERK proteins and glucose consumption rate. Also osteogenic differentiation efficiency was identified by determining calcium deposition, alizarin red staining, ALP activity and osteopontin and osteocalcin gene expression during culture expansion under conditions approved for clinical use.

The cell density of expansion with different confluences were as expected. It was noticed that the highest cell density appeared when the cell achieved

100% confluence and the lowest one appeared at 20% confluence. At 70% and 80% confluence, density was significantly lower than that at 100% confluence and higher than 20% confluence. Therefore, there was a correlation between confluences % and the cell density. BMMSCs viability was declined at lower and higher confluences and there is no significant difference in viability between 20% and 100% confluence. Previously, studies agree that there is no identical method for culturing MSC and no standards for degree of confluence, cell densities and duration of cell expansion. Some studies proposed that culturing cells at low density resulted in more rapid proliferation (Colter et al., 2000 and Sekiya et al., 2002). Others have noticed that keeping of very low cell densities through expansion was required to obtain homogeneous cell cultures with high proliferation and differentiation potential (Reyes et al., 2001 and Jiang et al., 2002). Ren et al. (2015) reported that growing BMMSCs to higher confluences was associated with increased cell density and yields, but this high degree was detrimental to MSC that impaired self-renewal and differentiation capacity, supporting the hypothesis that cell-to-cell contact is harmful to MSC quality. BMSCs grown to 50% confluence also differ from 80% confluent cells, but these differences were less certain. On that way, Song et al. (2009) showed that total cell numbers and density increased with time, but after that, the higher density cultures expanded more slowly accompanied with high apoptosis levels.

Concerning CFU-F, the results obtained revealed that as the confluence of BMMSCs increase until reach 80%, the cells become highly able to form CFU-F, followed by decrease. This data enforces other work⁴ who reported that confluence affected BMSC colony formation, particularly for 100% confluent cells. The quantity of colonies formed by BMSCs was similar for 50% and 80% confluent cells but was less for 100% confluent cells. In addition, these data agree to some extend with other work (Neuhuber et al., 2008) who observed the dense colonies at low plating density and cell growth was likely to be inhibited at the colony center because of contact inhibition. At intermediate density, the growth pattern was a mix of colonies. Gregory et al. (2005) suggested that avoiding overcrowding at the colony center might affect proliferation directly or indirectly through the induction of early differentiation of MSC.

The proliferation rate of BMMSCs at different confluences was assessed by Brd-U incorporation for 24 hours. The Brd-U uptake rate was significantly elevated as the confluence increased until reach 80% confluence followed by decrease at 100% confluence. The massive inhibition of proliferation rate with high confluences obtained in this work was previously

obtained (Both et al., 2007) who found that BMMSCs plated at lower densities had a faster proliferation than higher densities, a similar relationship was found (Lode et al., 2008) when they investigated the effect of seeding density on scaffolds. They reported that the highest seeding density of cells was resulted in a slight increase in cell number compared to the lowest seeding density, which had a large increase in cell number. In addition, Colter et al. (2000) reported that extremely low densities (0.5–12 cells/cm²) showed the size of single-cell-derived colonies that represent cell number and hence proliferation rate, to be inversely proportional to seeding density (Fossett and Khan, 2012).

The results of the population doubling showed that 70% and 80% confluences exhibit a significant increase in PDs when compared to that at 50% and 100% confluences. In most confluent BMMSCs, cell growth arrested in Passage 12–13, whereas 70% and 80% confluent proliferation stopped in Passage 14–16. Another study (Bartmann et al., 2007) seeded the BMMSCs at four different densities also had consistent results to these findings. They showed that seeding at lower density result in faster proliferation rate and PDs than those of a higher density. They also showed that cell characterization did not affected by seeding density as all cells had the same cell surface marker profiles. Another study explored the optimum seeding density for MSCs derived from different sources (Mochizuki et al., 2006). Seeding density as a factor beside age of donor and gender was affected proliferation rate and expansion of MSCs for clinical application (Fossett and Khan, 2012). They found that MSCs from a range of sources have a faster proliferation rate/PDs at lower seeding densities. Recently, PDT fell from 50% to 80% confluence and then increased when they became 100% confluent.⁴

The confluence-associated proliferation was provided by measuring bands of ERK and its phosphorylation (P-ERK) by Western blot. Bands of ERK were expressed among all the BMMSCs confluences while bands of P-ERK were highly detectable in 70% and 80% confluent BMMSCs than other confluences. Densitometric measures of band intensities found that ERK band intensity of 100% confluent BMMSCs was lower compared to other confluences. The intensities of remaining confluences bands were nearly the same. While the higher P-ERK band intensity was found in 70% and 80% confluent BMMSCs compared to other confluences. P-ERK in 80% confluent BMMSCs was much higher than 20% and 50% confluent cells but slightly higher than 70% and 100% confluent cells. P-ERK in 70% and 100% was higher than 20% and 50% confluences. These data are parallel to other data identify the cell proliferation and differentiation. Activated ERK

phosphorylates cellular substrates, many of which are kinases whose activity prolong and proliferate the signaling cascade (Jean-Claude et al., 2007). Also, phosphorylation might play a pivotal role in the regulation of cell proliferation and differentiation (Iván et al., 2008).

To identify signs other than microscopically identification of BMSC confluences, levels of glucose uptake by cells were measured in culture supernatants. All BMMSCs at all confluences are regular in glucose consumption after day 2. However, on days 3, 4 and 6, glucose consumption at 70% and 80% confluence was elevated than the others. On the day 5 the consumption rates at confluence 50, 70, and 80% were higher than the lowest (20%) and highest (100%) confluences. On the basis of these data, we concluded that the value of glucose is a good indicator of cell number and can be used to determine the timing of BMSC passage or harvest as previously mentioned (Ren et al., 2015).

Finding the optimum confluences for maximal osteogenic differentiation efficiency is useful in potential clinical applications. Calculation of the total area of Alizarin Red staining showed that BMMSCs approaching 20% and 50% confluence showed very low area of staining that indicating deficiency of in vitro osteogenic differentiation potential. 80% and 100% confluent BMMSCs showed higher staining than other confluences. Measurement of calcium deposition resulted in a significant increase in BMMSCs cultured to 80% confluence than both 70% and 100% confluence. BMMSCs cultured to 100% confluence recorded increase in the activity of ALP than other confluences. Expression of osteopontin gene was found among all confluences. In contrast, osteocalcin gene expression was abundant in 70% and 100% confluent cells than others. Collectively, most markers of osteogenic differentiation are increased with the increasing % confluence even at 100%. These data are in the agreement with others who worked in heterogeneous MSC populations (Neuhuber et al., 2008) or influence MSC phenotype during expansion (Gnecchi et al., 2005, Lu et al., 2009 and Haack-Sorensen et al., 2013).

On the contrary, seeding density has been shown to impact the efficiency of in vitro adipogenesis (Lu et al., 2009) chondrogenesis (Nakahara et al., 1991 and Seghatoleslami and Tuan, 2002) osteogenesis (Gao et al., 2010 and Kilian et al., 2010) or myofibroblastogenesis (Sotiropoulou et al., 2006). They recorded that poor differentiation of varying MSC types at high seeding density could be due to mechanical factors (Sekiya et al., 2002, Sotiropoulou et al., 2006 and Gao et al., 2010). It was previously demonstrated that in vivo bone formation ability of 100% confluent BMSCs was reduced compared with

70% confluent BMSCs, but this difference was donor dependent (Kuznetsov et al., 2000 and Balint et al., 2015). They concluded that the low density cultures give valuable effects while high confluence cultures was resulted in reduced osteogenic and adipogenic differentiation. Ren et al. (2015) showed that harvesting cells at 80% confluence was optimal because most bone biomarkers gene expression was changed in 100% confluent cells suggesting that the genes that were up regulated in 100% confluent BMSCs were inhibitor genes and angiogenesis inhibitors.

The data concluded that 80% confluence is the best than extremely low or high density for proliferation or osteogenic differentiation. Previous studies collectively attributing that to the contact inhibition. The effect of confluence could possibly be different when grow BMMSCs under other conditions or isolation of MSCs from other tissues. For example, it is not known if the effect of confluence would be the same when BMMSCs grown in bioreactors or scaffold, with other media such as serum free culture media or on other types or sources of stem cells. In addition, the effects of confluence on the in vivo properties of BMMSCs could differ from the properties measured in vitro. Unfortunately, these literatures not answered what about the time needed to cells to take amount of nutrition from media to become powerful to have the ability for differentiation. What is the exact confluence of cells to gain the natural shape to be able to differentiate? What is the exact confluent cell to communicate with other cells? What is the exact confluence to gain activating gene and surface receptors of cytokine and growth factors that capable for the work of differentiation? Answered these questions need further investigation.

Acknowledgements:

The corresponding author thanks the staff of Dr. Yamaza laboratory, Department of Molecular Biology and Oral Anatomy, Graduate School of Dental Science, Kyushu University, Fukuoka, Japan for their supplying with some materials and for gaining the experience about stem cells in their laboratory.

Corresponding Author:

Dr. Faten A.M. Abo-Aziza
Department of Parasitology and Animal Diseases,
Veterinary Research Division, National Research
Center (Cairo, Egypt).
Telephone: 0020-01005233692
E-mail: faten.aboaziza@gmail.com

References

1. Arash Z, Iraj RK, Mohammad B, Azim H, Reza M and Ahmadreza FN. Osteogenic Differentiation of Rat Mesenchymal Stem Cells from Adipose Tissue in Comparison with Bone Marrow Mesenchymal Stem Cells: Melatonin as a Differentiation Factor. *Iranian Biomedical J* 2008; 12 (3): 133-141.
2. Bae S, Ahn JH, Park CW, Son HK, Kim KS, Lim NK, et al. Gene and microRNA expression signatures of human mesenchymal stromal cells in comparison to fibroblasts. *Cell Tissue Res* 2009; 335: 565-573.
3. Balint R, Stephen MR and Sarah HC. Low-density subculture: a technical note on the importance of avoiding cell-to-cell contact during mesenchymal stromal cell expansion. *J Tissue Eng Regen Med* 2015; 9, 1200.
4. Barry FP. Biology and clinical applications of mesenchymal stem cells. *Birth Defects Res C Embryo Today* 2003; 69: 250–256.
5. Bartmann C, Rohde E, Schallmoser K et al. Two steps to functional mesenchymal stromal cells for clinical application. *Transfusion* 2007; 47, 1426.
6. Bittencourt R and Aparecida C, Isolation of bone marrow mesenchymal stem cells. *Acta ortop. Bras* 2006; 14 (1): 22-24.
7. Both SK, van derMuijsenberg AJC, van Blitterswijk CA, de Boer J and de Bruijn JD. Rapid and Efficient Method for Expansion of Human Mesenchymal Stem Cells. *Tissue Engineering* 2007; 13, 3.
8. Chandrasekhar KS, Zhou H, Zeng P, Alge D, Li W, Finney BA, Yoder MC, Li J. Blood vessel wall- derived endothelial colony-forming cells enhance fracture repair and bone regeneration. *Calcif Tissue Int* 2011; 89: 347-357.
9. Cho Y, Shin J, Kim H, Gerelmaa M, Yoon H, Ryoo H, Kim D and Han J. Comparison of the Osteogenic Potential of Titanium- and Modified Zirconia-Based Bioceramics. *Int. J. Mol. Sci* 2014; 15, 4442-4452.
10. Claes L, Recknagel S, Ignatius A. Fracture healing under healthy and inflammatory conditions. *Nat Rev Rheumatol* 2012; 8:133-143.
11. Colter D, Class R, DiGirolamo C, et al. Rapid expansion of recycling stem cells in cultures of plastic-adherent cells from human bone marrow. *Proc Natl Acad Sci U S A* 2000; 97: 3213–3218.
12. Corcione A, Benvenuto F, Ferretti E, Giunti D, Cappiello V, Cazzanti F, et al. Human mesenchymal stem cells modulate B-cell functions. *Blood* 2006; 107: 367-372.
13. Fossett E and Khan WS. Optimising Human Mesenchymal Stem Cell Numbers for Clinical Application: A Literature Review. *Stem Cells International* 2012; 465259.
14. Gao L, McBeath R and Chen CS. Stem cell shape regulates a chondrogenic versus myogenic fate through Rac1 and N-cadherin. *Stem Cells* 2010; 28, 564.
15. Gneccchi M, He H, Liang OD, et al. Paracrine action accounts for marked protection of ischemic heart by Akt-modified mesenchymal stem cells. *Nature Medicine* 2010; 11, 367.
16. Gneccchi, M., He, H., Liang, O. D., et al. Paracrine action accounts for marked protection of ischemic heart by Akt-modified mesenchymal stem cells. *Nature Medicine* 2005; 11(4): 367–368.
17. Gregory CA, Gunn WG, Peister A and Prockop DJ. An Alizarin red-based assay of mineralization by adherent cells in culture: comparison with cetylpyridinium chloride extraction. *Anal. Biochem* 2004; 329, 77-84.
18. Gregory CA, Ylostalo J, Prockop DJ. Adult bone marrow stem/progenitor cells (MSCs) are preconditioned by microenvironmental niches” in culture: a two-stage hypothesis for regulation of MSC fate. *Sci STKE* 2005; 294, 37.
19. Grisendi G, Anneren C, Cafarelli L, Sternieri R, Veronesi E, Cervo GL, et al. GMP-manufactured density gradient media for optimized mesenchymal stromal/stem cell isolation and expansion. *Cytotherapy* 2010; 12:466-477.
20. Haack-Sorensen M, Susanne K H, and Louise H, Michael G, Poul H, Annette E and Jens K. Mesenchymal Stromal Cell Phenotype is not Influenced by Confluence during Culture Expansion. *Stem Cell Rev and Rep* 2013; 9, 44.
21. Iván C, Naiara T, Jesús D, Ainhoa G, David O, Valerie L and César T. ERK2 protein regulates the proliferation of human mesenchymal stem cells without affecting their mobilization and differentiation potential. *Experimental Cell Research* 2008; 314, 1777–1788.
22. Jean-Claude C, Renaud L, Jacques P, Philippe L. ERK implication in cell cycle regulation. *Biochimica et Biophysica Acta* 2007; 1773,1299–1310.
23. Jeong JA, Ko KM, Bae S, Jeon CJ, Koh GY and Kim H. Genome-wide differential gene expression profiling of human bone marrow stromal cells” *Stem Cells* 2007; 25, 994-1002.
24. Jiang Y, Jahagirdar BN, Reinhardt RL, et al. Pluripotency of mesenchymal stem cells derived from adult marrow. *Nature* 2002; 418, 41.
25. Jones E, English A, Churchman SM, Kouroupis D, Boxall SA, Kinsey S, et al. Large-scale extraction and characterization of CD271p

- multipotential stromal cells from trabecular bone in health and osteoarthritis: implications for bone regeneration strategies based on uncultured or minimally cultured multipotential stromal cells. *Arthritis Rheum* 2010; 62, 1944-1954.
26. Kentaro A, Yong-Ouk Y, Takayoshi Y, Chider C, Liang T, Yan J, Xiao-Dong C, Stan G and Songtao S. Characterization of bone marrow derived mesenchymal stem cells in suspension. *Stem Cell Research & Therapy* 2012; 3, 40.
 27. Kilian KA, Bugarija B, Lahn BT and Mrksich M. Geometric cues for directing the differentiation of mesenchymal stem cells. *Proc. Natl. Acad. Sci. USA* 2010; 107, 4872.
 28. Kinnaird T, Stabile E, Burnett MS, et al. Marrow-derived stromal cells express genes encoding a broad spectrum of arteriogenic cytokines and promote in vitro and in vivo arteriogenesis through paracrine mechanisms” *Circulation Research* 2004; 94, 5, 678–685.
 29. Koc ON, Gerson SL, Cooper BW, Dyhouse SM, Haynesworth SE, Caplan AI, et al. Rapid hematopoietic recovery after coinfusion of autologous-blood stem cells and culture-expanded marrow mesenchymal stem cells in advanced breast cancer patients receiving high-dose chemo- therapy. *J Clin Oncol* 2000; 18: 307-316.
 30. Kuznetsov SA, Mankani MH, Robey PG. Effect of serum on human bone marrow stromal cells: ex vivo expansion and in vivo bone formation” *Transplantation* 2000; 70, 1780.
 31. Lazarus HM, Koc ON, Devine SM, Curtin P, Maziarz RT, Holland HK, et al, Cotransplantation of HLA-identical sibling culture-expanded mesenchymal stem cells and hematopoietic stem cells in hematologic malignancy patients. *Biol. Blood Marrow Transplant* 2005; 11: 389-398.
 32. Lee J, Suh J, Park H, Bak E, Yoo YJ, and Cha JH. Heparin-binding epidermal growth factor-like growth factor inhibits adipocyte differentiation at commitment and early induction stages. *Differentiation* 2008; 76, 5, 478-487.
 33. Lilian PE, Renata BR, Isis SO, Paulo OG, Paulo P, Alice TF, Marcelo PV. Comparative study of technique to obtain stem cells from bone marrow collection between the iliac crest and the femoral epiphysis in rabbits. *Acta Cirúrgica Brasileira* 2009; 24, 5, 400.
 34. Liu BS, Yao CH, Chen YS, and Hsu SH. In vitro evaluation of degradation and cytotoxicity of a novel composite as a bone substitute. *J Biomed Mat Res* 2003; 67, 4: 1163–1169.
 35. Liu J, Zhao Z, Li J, Zou L, Shuler C, Zou Y, Huang X, Li M, and Wang J. Hydrostatic Pressures Promote Initial Osteodifferentiation with ERK 1/2 Not p38 MAPK Signaling Involved. *J Cellular Biochem* 2009; 107, 2, 224-232.
 36. Lode A, Bernhardt A and Gelinsky M. Cultivation of human bone marrow stromal cells on three-dimensional scaffolds of mineralized collagen: influence of seeding density on colonization, proliferation and osteogenic differentiation. *J Tiss Eng Reg Med* 2008; 2, 400.
 37. Lu H, Guo L, Wozniak MJ, Kawazoe N, Tateishi T, Zhang X et al. Effect of cell density on adipogenic differentiation of mesenchymal stem cells. *Biochem. Biophys. Res. Commun* 2009; 381, 322.
 38. Mandana H, Susanne K, Louise H, Michael G, Poul H, Annette E and Jens K. Mesenchymal Stromal Cell Phenotype is not Influenced by Confluence during Culture Expansion. *Stem Cell Rev and Rep* 2013; 9, 44–58.
 39. Mankani MH, Kuznetsov SA, Marshall GW and Robey PG. Creation of new bone by the percutaneous injection of human bone marrow stromal cell and HA/TCP suspensions” *Tissue Eng Part A* 2008; 14, 1949-1958.
 40. Mochizuki T, Muneta T, Sakaguchi Y et al. Higher chondrogenic potential of fibrous synovium- and adipose synovium-derived cells compared with subcutaneous fat-derived cells: distinguishing properties of mesenchymal stem cells in humans. *Arthritis and Rheumatism* 2006; 54, 843.
 41. Nakahara H, Goldberg VM and Caplan AI. Culture-expanded human periosteal-derived cells exhibit osteochondral potential in vivo. *J. Orthop. Res* 1991; 9, 465.
 42. Neuhuber B, Sharon AS, Linda H, Alastair M, and Itzhak F. Effects of Plating Density and Culture Time On Bone Marrow Stromal Cell Characteristics. *Exp Hematol* 2008; 36, 1176.
 43. Palaez D, Arita N, and Cheung H. Extracellular signal-regulated kinase (ERK) dictates osteogenic and/or chondrogenic lineage commitment of mesenchymal stem cells under dynamic compression. *Biochem Biophys Res Comm* 2012; 417, 4, 1286-1291,.
 44. Prockop DJ, Gregory C, Spees JL. One strategy for cell and gene therapy: harnessing the power of adult stem cells to repair tissues. *Proc Natl Acad Sci U S A* 2003;100 (1):11917- 11923.
 45. Ren J, Huan W, Katherine T, Sara C, Ping J, Luciano C, Ji F, Sergei A K, Pamela GR, Marianna S and David FS. Human bone marrow

- stromal cell confluence: effects on cell characteristics and methods of assessment” *Cytotherapy* 2015; 17, 897-911.
46. Reyes and M, Verfaillie CM. Characterization of multipotent adult progenitor cells, a subpopulation of mesenchymal stem cells” *Ann N Y Acad Sci* 2001; 938, 231–233.
 47. Roman MS, Robert FK, Mariah KH and George EP. ERK Signaling Pathways Regulate the Osteogenic Differentiation of Human Mesenchymal Stem Cells on Collagen I and Vitronectin” *Cell Communication and Adhesion* 2004; 11,137–153.
 48. Röntgen V, Blakytyn R, Matthys R, Landauer M, Wehner T, Göckelmann M, et al. Fracture healing in mice under controlled rigid and flexible conditions using an adjustable external fixator. *J Orthop Res* 2010; 28,1456-1462.
 49. Rosova I, Dao M, Capoccia B, Link D and Nolte JA. Hypoxic preconditioning results in increased motility and improved therapeutic potential of human mesenchymal stem cells. *Stem Cells* 2008; 26, 2173-2182.
 50. Salasznyk RM, Klees RF, Hughlock MK, Plopper GE. ERK signaling pathways regulate the osteogenic differentiation of human mesenchymal stem cells on collagen I and vitronectin. *Cell Commun Adhes* 2004; 11,137–153.
 51. Samuelsson H, Ringden O, Lonnie H and Le Blanc K. Optimizing in vitro conditions for immunomodulation and expansion of mesenchymal stromal cells. *Cytotherapy* 2009; 11, 129-136.
 52. Seghatoleslami MR and Tuan RS. Cell density dependent regulation of AP-1 activity is important for chondrogenic differentiation of C3H10T1/2 mesenchymal cells. *J. Cell. Biochem* 2002; 84, 237-248.
 53. Sekiya I, Larson BL, Smith JR, et al. Expansion of human adult stem cells from bone marrow stroma: conditions that maximize the yields of early progenitors and evaluate their quality. *Stem Cells* 2002; 20, 530–541.
 54. Song I Arnold IC and James ED. Dexamethasone Inhibition of Confluence-Induced Apoptosis in Human Mesenchymal Stem Cells. *Inc. J Orthop Res* 2009; 27, 216.
 55. Sotiropoulou P, Perez S, Salagianni M, et al. Characterization of the optimal culture conditions for clinical scale production of human mesenchymal stem cells. *Stem Cells* 2006; 24, 462,.
 56. Tahrin M and Ping-Chang Y. Western Blot: Technique, Theory, and Trouble Shooting. *N Am J Med Sci* 2012; Sep, 4, 9, 429–434.
 57. Tain-Hsiung C, Wei-Ming C, Ke-Hsun H, Cheng-Deng K and Shih-Chieh H. Sodium butyrate activates ERK to regulate differentiation of mesenchymal stem cells. *Biochem Biophys Res Comm* 2007; 355, 913–918.
 58. Tormin A, Brune JC, Olsson E, Valcich J, Neuman U, Olofsson T, et al. Characterization of bone marrow-derived mesenchymal stromal cells (MSC) based on gene expression profiling of functionally defined MSC subsets. *Cytotherapy* 2009; 11:114-128.
 59. Waters, WR, Palmer MV, Whipple DL, Carlson MP and Nonnecke BJ. Diagnostic implications of antigen-induced gamma interferon, nitric oxide and tumor necrosis factor alpha production by peripheral blood mononuclear cells from mycobacterium bovis-infected cattle. *Clin Diag Lab Immun* 2003; 10, 960-966.
 60. Wen JH, Vincent LG, Fuhrmann A, Choi YS, Hribar KC, Taylor-Weiner H, Chen S, and Engler AJ. Interplay of matrix stiffness and protein tethering in stem cell differentiation. *Nature Materials* 2014; 13, 10, 979-987.
 61. Wolfe M, Pochampally R, Swaney W and Reger RL. Isolation and Culture of Bone Marrow-Derived Human Multipotent Stromal Cells (hMSCs). *Methods Mol Biol* 2008; 449, 3-25.
 62. Zhukareva V, Obrocka M, Houle JD, Fischer I and Neuhuber B. Secretion profile of human bone marrow stromal cells: donor variability and response to inflammatory stimuli. *Cytokine* 2010; 50, 317-321.

9/22/2016